MAVEN SOFTWARE INC.
+1 305 450 1295 | andrew@hustrulid.com

Steel Cord Splice Xray and FEA Report

Customer xyz | ST2800 belt | 1,828 mm width | 105 parent cords

Prepared by Andrew I. Hustrulid, PhD, PE

Summary of findings

This assessment compares the as-constructed layout interpreted from the Customer xyz splice X-ray with an as-designed reference generated in SteelCordSplice, using two-dimensional finite element analysis (FEA). The as-designed reference has both outer cords pointing in the confirmed direction of belt travel.

The highest sampled cord tension is 1.84 times the equal share as constructed, compared with 1.44 as designed, an increase of 27.5%. The as-constructed case has a calculated center of tension 62.7 mm left of the belt center. Rubber shear p95 is 10.2% above the as-designed case, while p99 is 19.1% higher.

X-ray estimates give a 19.4 degree bias from across the belt, steps of about 640 and 620 mm, and a median short-cord end gap of 53 mm.

Calculated results at a common load

Measure	As designed	As constructed spacing adjusted
Maximum sampled cord tension / equal share	1.44 times	1.84 times*
Rubber shear p95	0.001178 MPa	0.001299 MPa
Rubber shear p99	0.001455 MPa	0.001733 MPa
Center of tension at the middle section	2.9 mm left	62.7 mm left

** The 1.84 maximum occurs on cord B104. All results use 1 kN total belt tension; they are model outputs, not measured operating loads.*

Assessment basis

As designed denotes the expected reference layout, not a manufacturer-approved drawing. As constructed denotes the X-ray-based model, including inferred routes and local spacing adjustments. Both use a provisional 7.6 mm cord diameter and assumed image scale. These comparative results do not establish splice strength, remaining life or measured belt mistracking.

Splice Xray

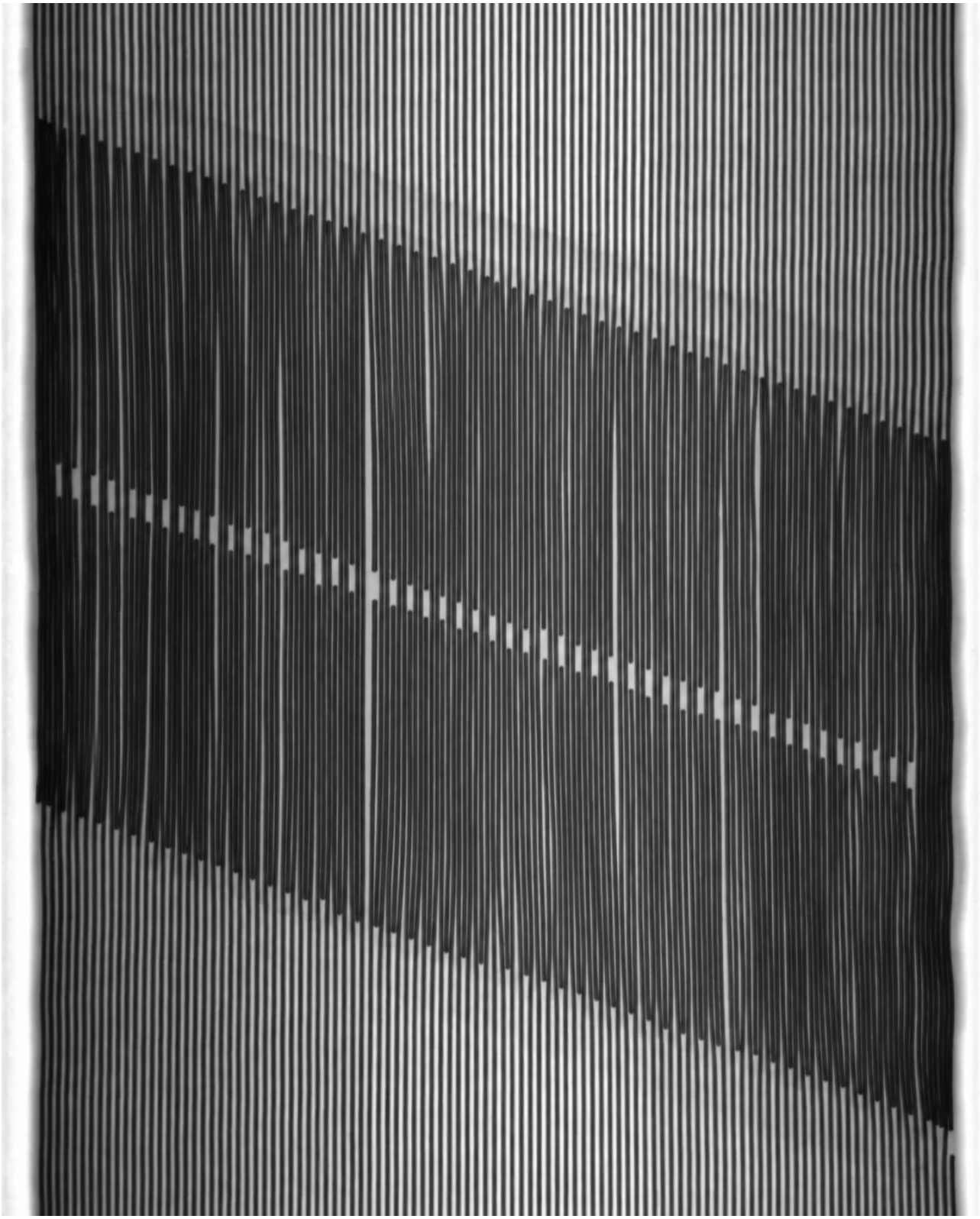

Figure 1. Illustrative X-ray reconstruction. Reconstructed detail is inferred; cord identification, measurements and FEA use the original X-ray.

Cord identification

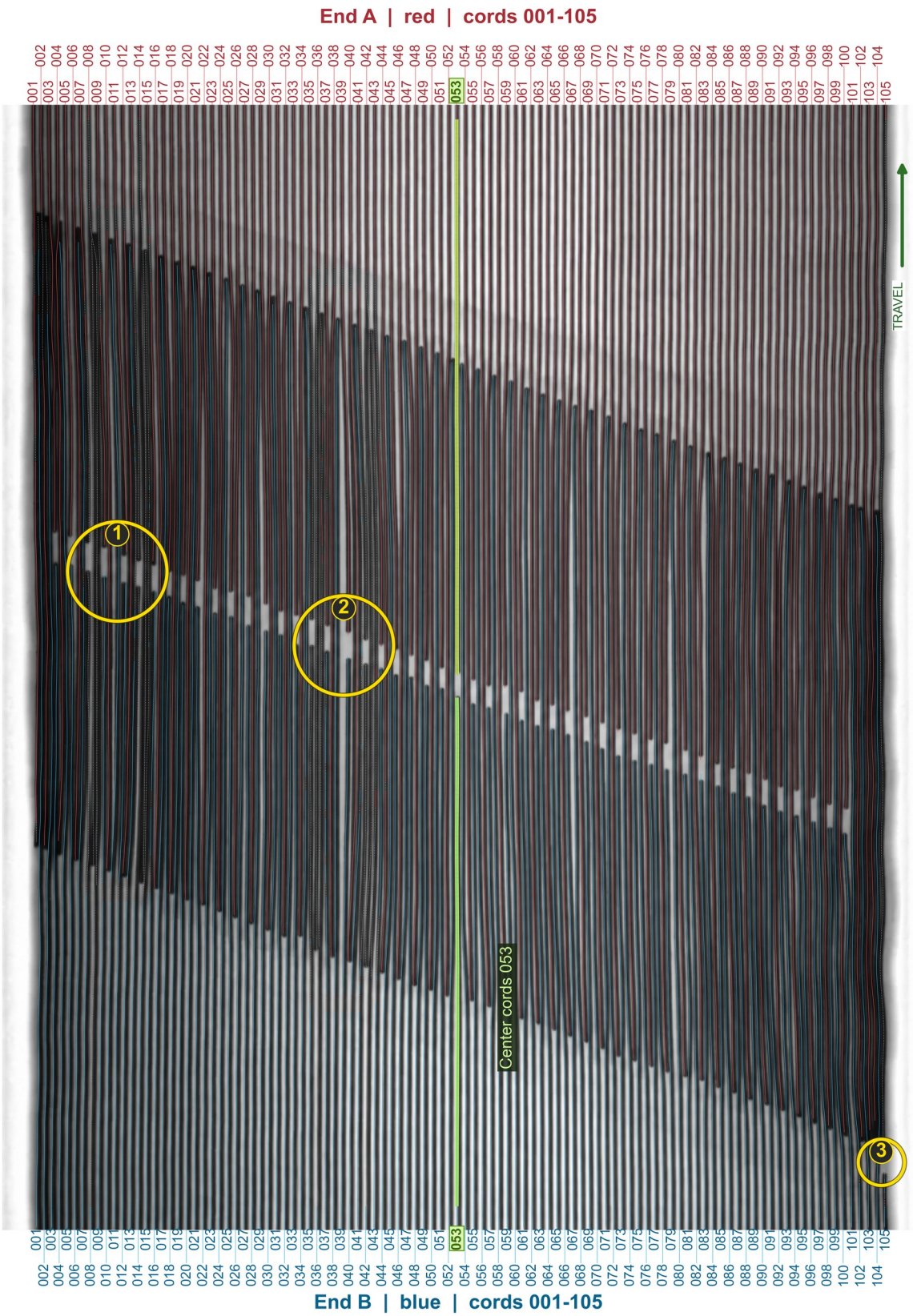

Figure 2. Original X-ray cord paths over the cleaned illustration. A001-A105 enter from above; B001-B105 from below. Green marks center cords 053; gray dashed paths are uncertain. Yellow circles locate the details below.

Cord count and pattern review

The X-ray shows 105 cords at each parent-belt end, with all 210 paths numbered. This confirms the parent count; it does not confirm every route through the splice. Of the 210 paths, 164 have no flagged intervals, 40 are partly flagged and 6 are flagged throughout.

Routes flagged throughout: A008, A014, A105, B008, B036, B042. Their through-splice continuity cannot be independently resolved in this image.

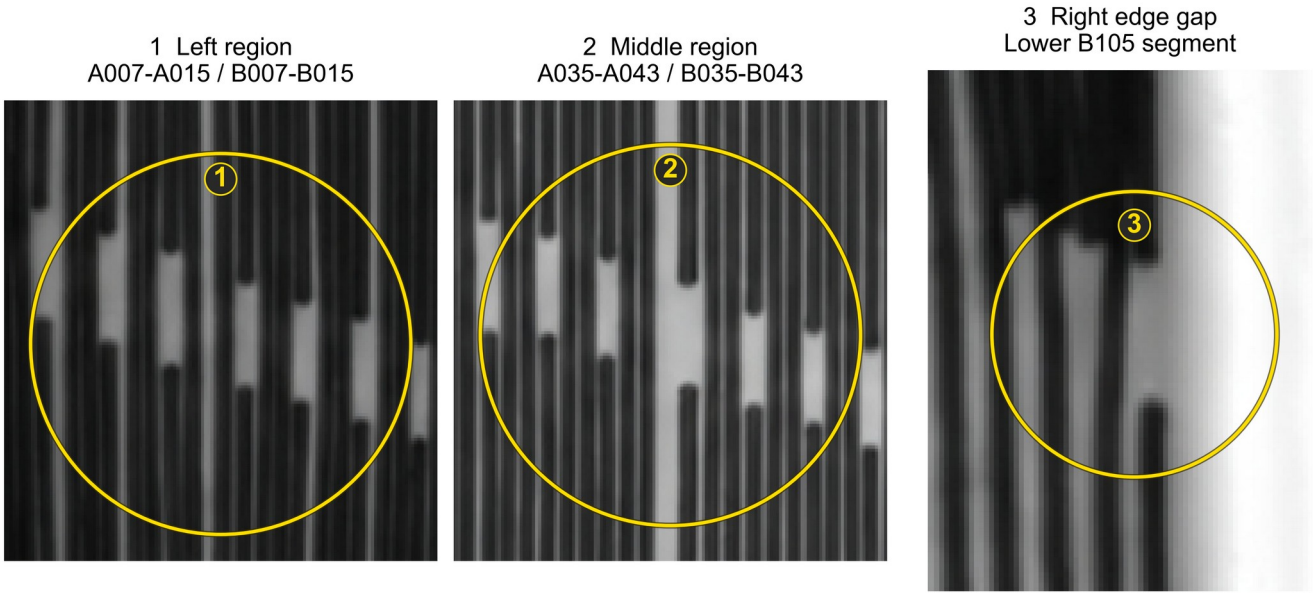

Figure 3. Enlarged cleaned illustration. Yellow circles locate irregularities identified in the original X-ray; the ranges refer to the numbered map.

Center repeats and edges

Location	Finding against the as-designed reference
Center	The opposing short-cord pair A053/B053 is correct. The neighboring long cords are B052/B054 as constructed; the as-designed layout places A052/A054 next to center. The surrounding cord order therefore differs.
Repeats on each side	As designed, there are 26 three-lane repeats to each side of center. The as-constructed interpretation has 25 recognizable groups on the left and 24 on the right, followed by irregular edge groups. These counts do not mean every group is correctly laid out.
Left edge	Appears incorrect. The as-constructed interpretation places A001 outermost, pointing against belt travel, instead of the required long B cord. Low contrast leaves parts of A001/B001 inferred.
Right edge	The expected continuous long B105 edge cord is not present in the traced layout. A visible gap separates its lower segment from an upper segment of unresolved identity. The adjacent long-cord grouping also differs.

A repeat comprises one long A cord, one long B cord and an opposing short-cord pair in three lanes. Twelve of the 25 left-side groups include inferred intervals.

Circles 1 and 2 show uneven spacing and short-cord end alignment around A007-A015 / B007-B015 and A035-A043 / B035-B043. Circle 3 marks the right-edge gap. Close projected paths do not establish physical contact.

Splice bias and step lengths

Customer xyz | X-ray dimensions

1,828 mm belt width | 105 parent cords | travel direction shown

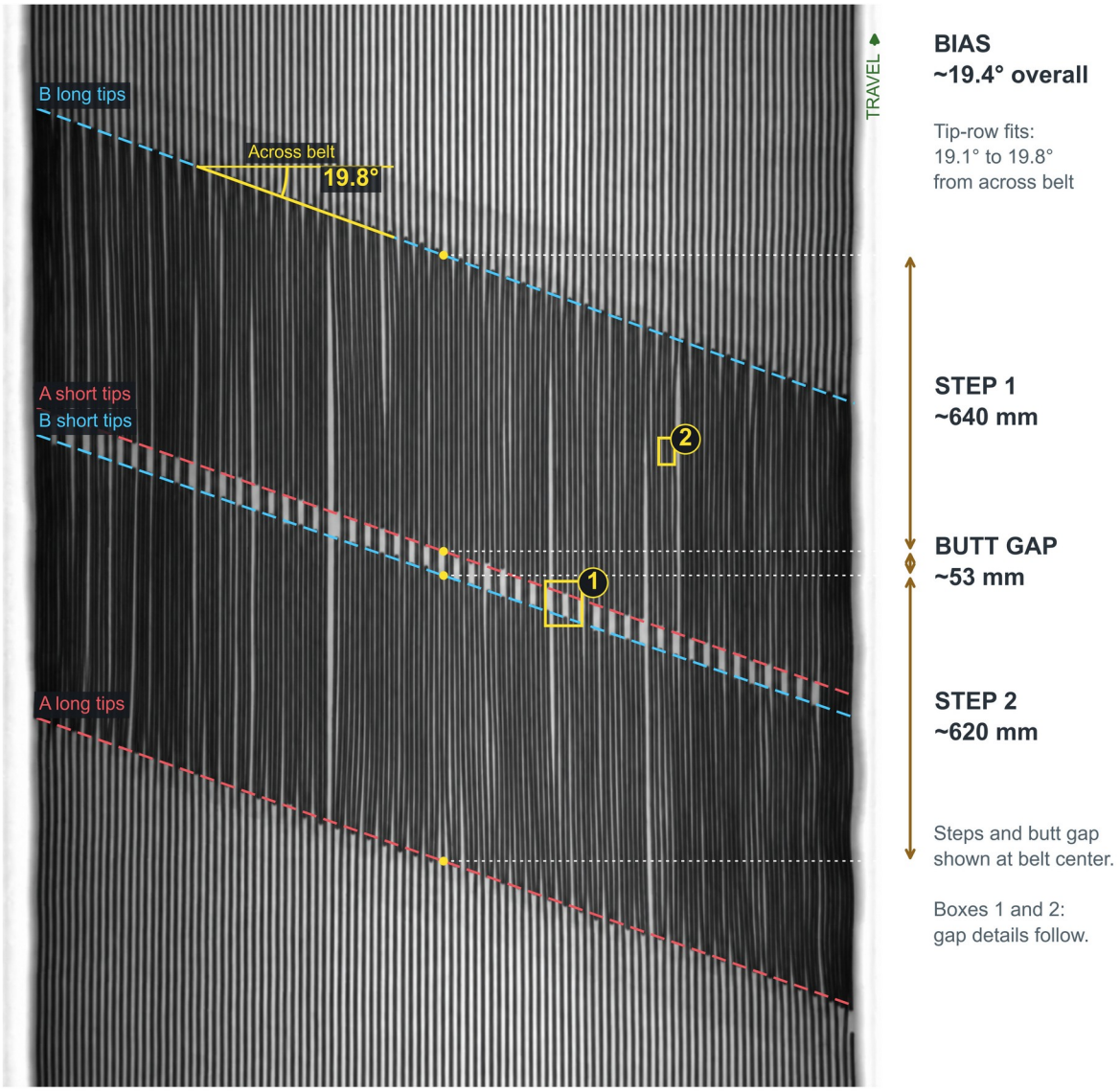

Step dimensions follow the belt length. Dashed lines fit the original X-ray cord-tip rows.

Scale: 2.407 mm/pixel from parent-cord span, using 25 mm edge rubber and 7.6 mm cord diameter.

Dimensions are approximate; equal transverse/longitudinal image scale is assumed. Cord gaps vary locally.

Figure 4. Original X-ray measurements over the cleaned illustration. Steps and the butt gap follow the belt length at its center; the bias angle is measured from across the belt.

Cord gap dimensions

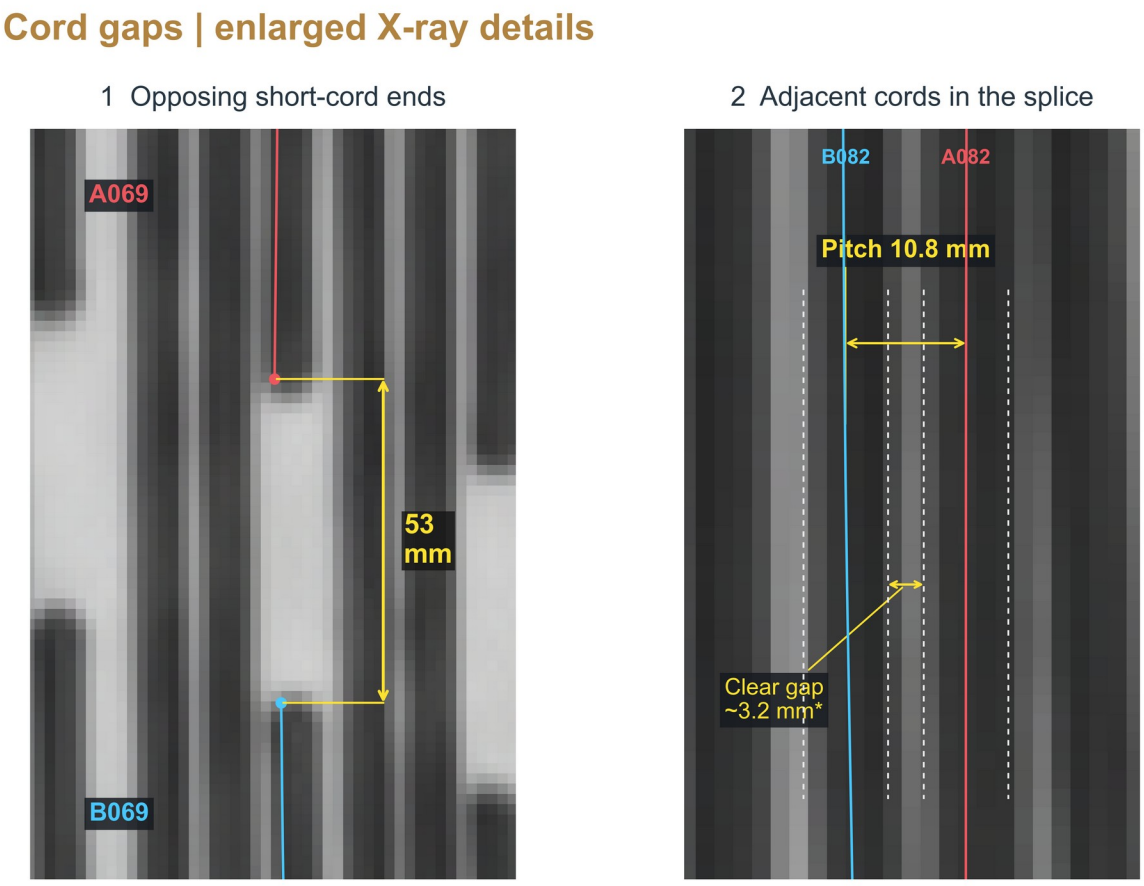

*Clear side gap = center pitch - 7.6 mm provisional cord diameter.

White dashed edges show that diameter assumption; actual cord edges are not resolved precisely.

These are local examples. Across the sampled splice: median pitch ~10.8 mm; median butt gap ~53 mm.

Figure 5. Original X-ray gap measurements over the cleaned illustration. White dashed edges use the provisional cord diameter; the background contains inferred detail.

Dimension	Approximate X-ray estimate
Bias angle from the transverse direction	19.4 degrees
Upper / lower axial step at belt center	640 / 620 mm
Opposing short-cord end gap (median)	53 mm
Cord pitch within the splice (median)	10.8 mm
Clear side gap (pitch minus assumed diameter)	3.2 mm

The four fitted tip rows range from 19.1 to 19.8 degrees. The 5th to 95th percentile end-gap range is 43 to 63 mm across 40 paired short-cord ends.

Dimensions assume 25 mm edge rubber, a 7.6 mm cord diameter and equal transverse and longitudinal image scale. One source pixel is about 2.4 mm. Clear side gap is a diameter-dependent estimate.

FEA splice model

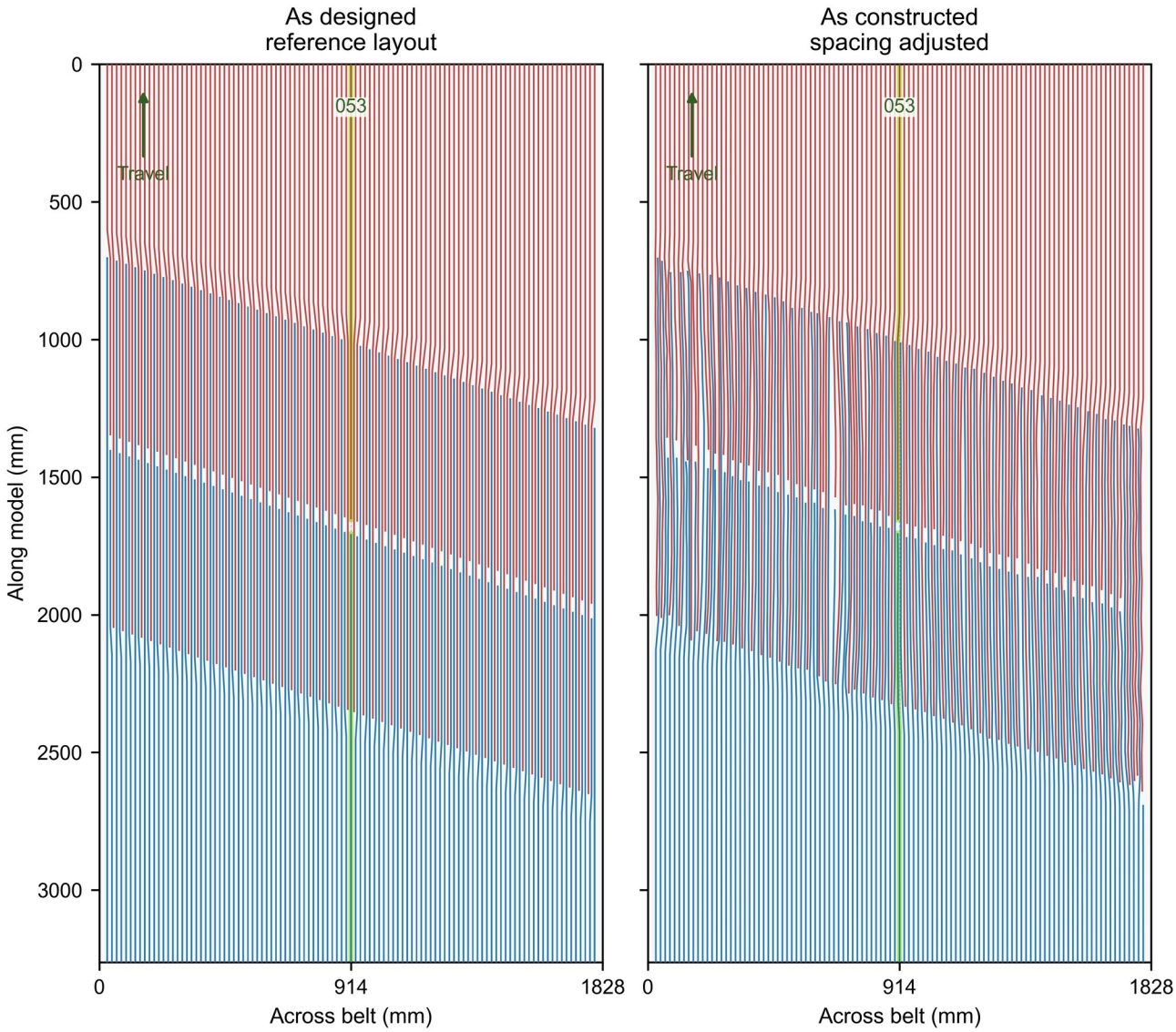

Figure 6. As designed and as constructed. Red: end A. Blue: end B. Green highlights center cords A053/B053. As designed, long cords B001/B105 occupy both outside edges and point with belt travel.

The as-designed layout has a central short-cord pair and 26 three-lane repeats on each side: 157 lanes in total. From center outward, each repeat is long A, a short A/B pair, then long B. This places long B cords at both edges, pointing with belt travel. The as-constructed interpretation predominantly repeats long B, long A, then a short pair, with irregular edge groups.

The as-constructed model includes the visible B105 lower segment and retains the uncertain upper route as an A105 modeling assumption. Local spacing changes reach 3.93 mm. Both models use a 7.6 mm core, 5.969 mm strips, nominal 100 mm transitions and 500 mm added parent lengths.

Tension in the cords

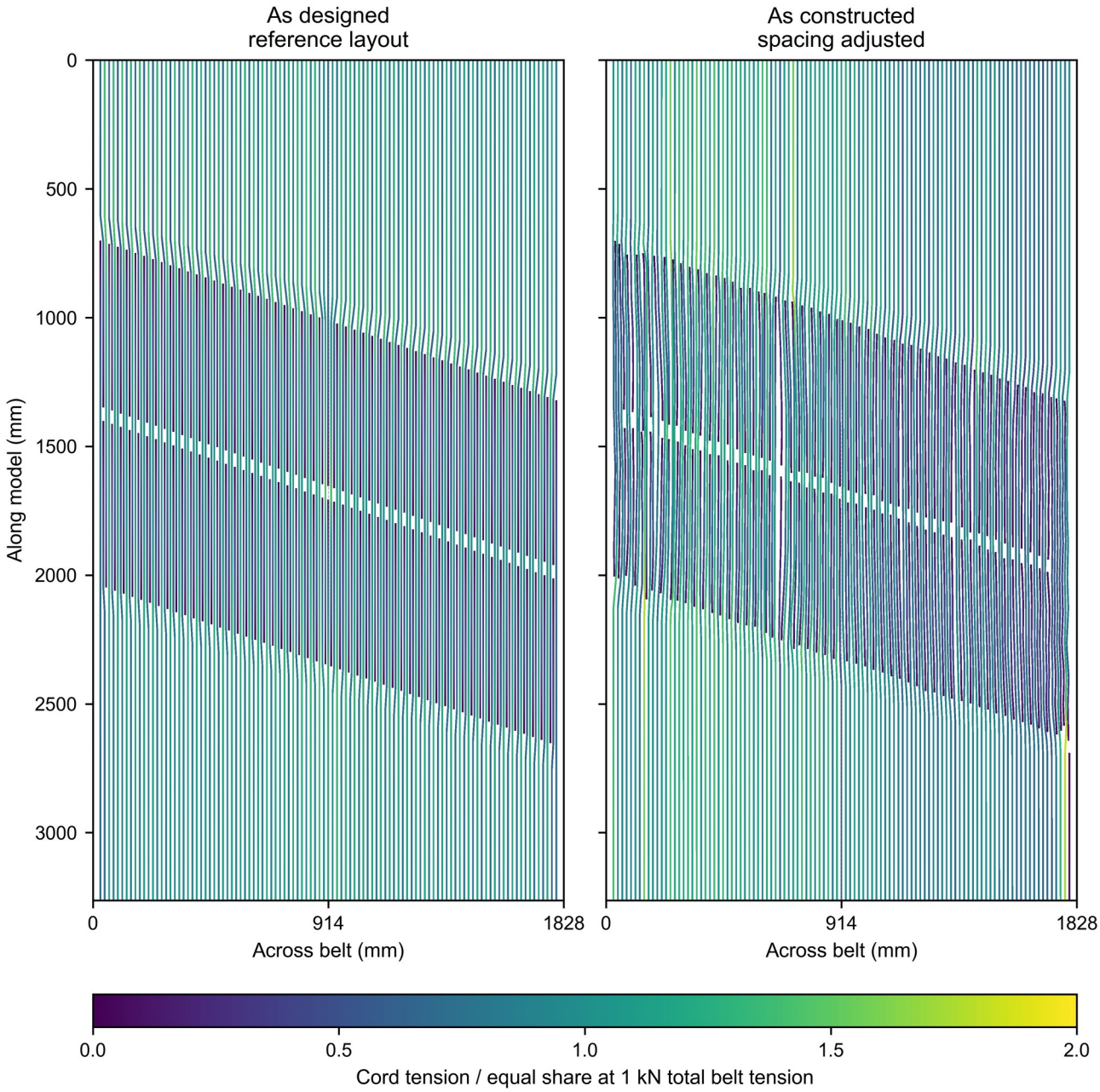

Figure 7. Calculated cord tensions on a common color scale. A value of 1.0 equals 9.524 N per cord at the 1 kN reference load.

The highest sampled cord tension as constructed is 1.84 times the equal share, or 84% above equal loading. This is 27.5% higher than the as-designed maximum of 1.44 times the equal share. The 1.84 maximum occurs on cord B104.

These maps locate load concentrations in the assumed geometry. They do not represent measured forces or a strength rating for an individual cord.

Shear transfer through the rubber

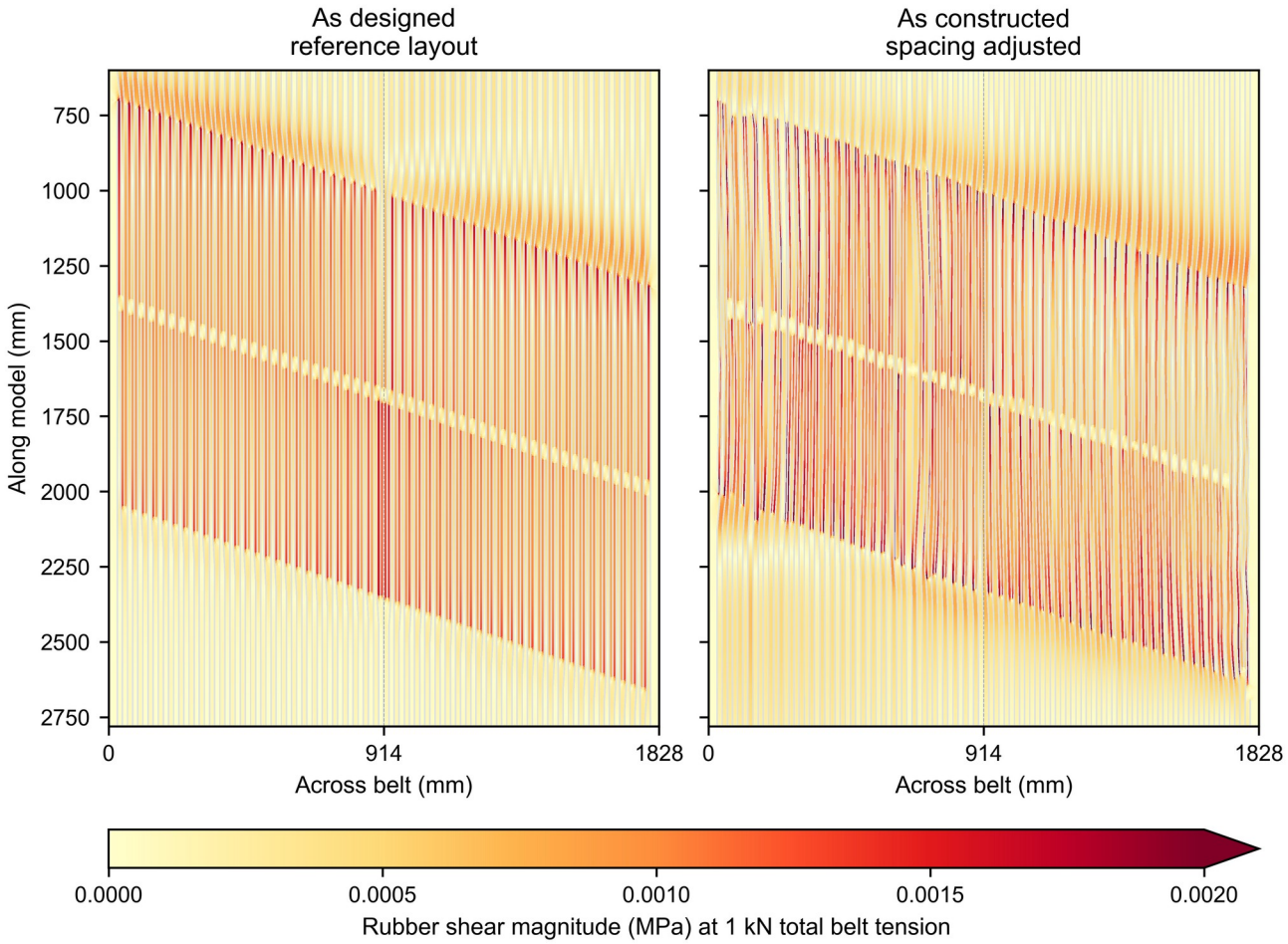

Figure 8. Rubber shear on a common 0 to 0.002 MPa scale at 1 kN total belt tension. Values above the scale saturate; gray regions are cord strips.

Rubber shear p95 is 10.2% higher as constructed than as designed; p99 is 19.1% higher. These area-weighted percentiles describe the stress below which 95% and 99% of the assessed rubber area falls. The contrast shows where the layout changes the local load-transfer pattern.

Model basis and checks

The calculation assumes linear elasticity and perfect bonding: rubber modulus 6 MPa and effective cord modulus 99.37 GPa. Diameter trials from 7.3 to 8.0 mm gave as-constructed model offsets from -63.2 to -62.5 mm. Refining the mesh changed extension and shear p95 by at most 0.27%.

The provisional diameter is based on the required 48.75 kN breaking load per cord and a published reference construction. Longitudinal scale is assumed from the image width. Local tip peaks and unresolved routes remain model limitations.

Sources: case X-ray reconstruction and saved FEA results, September 2026; Metso Conveyor Solutions Handbook (reference cord-strength table).

Load balance and the tracking indicator

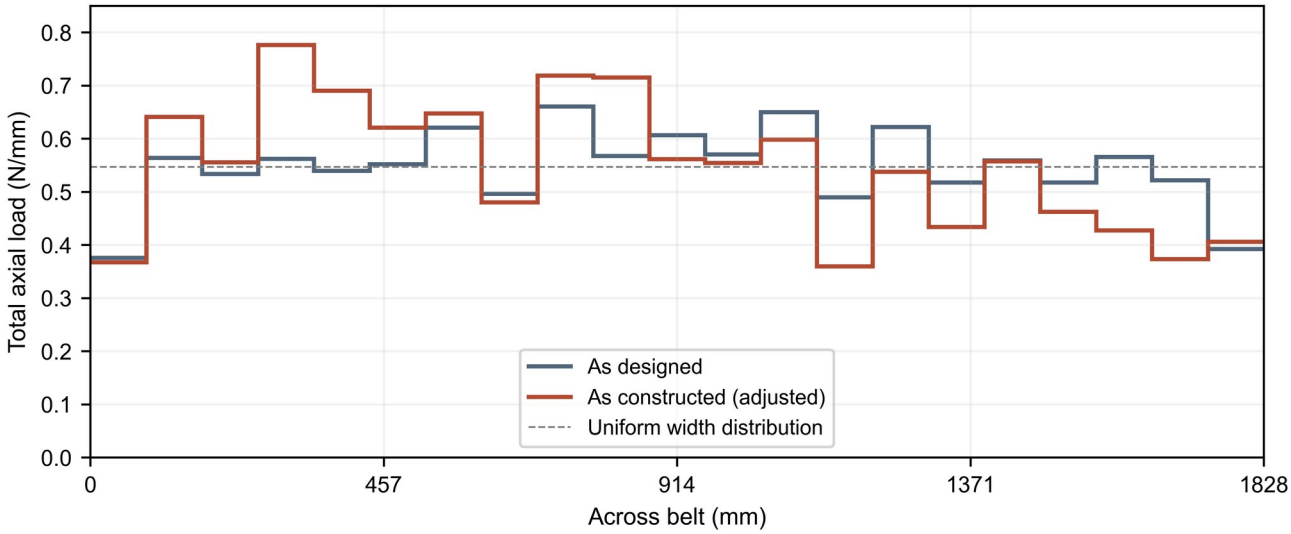

Figure 9. Steel and rubber tension across the width at the middle section. Both cases use 1 kN total belt tension.

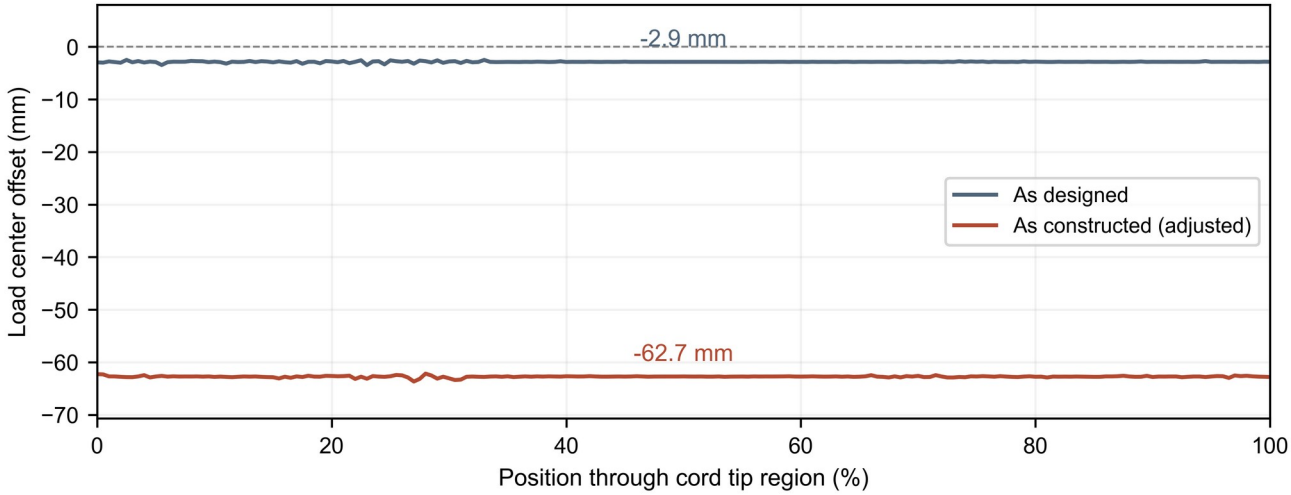

Figure 10. Calculated center of tension through the cord-tip region. Negative values are left in the X-ray view; the belt centerline is 914 mm from the left edge.

At the middle section, the as-constructed model carries 56.1% of the axial load in the left half of the belt. Its center of tension is 62.7 mm left of center, compared with 2.9 mm left as designed.

This offset serves as a tracking indicator of static load asymmetry. It depends on the modeled layout and end restraints; it does not predict lateral belt travel, tracking direction or the timing of a tracking event.